TRANSACTIONS OF THE CHINESE SOCIETY FOR AGRICULTURAL MACHINERY
Vol. 47, No. 9, 2016

doi:10.6041/j. issn. 1000-1298. 2016. 09. 039

Simulation on Ecological Land Use Expansion Based on EnKF – MCRP Model

Yu Qiang[1] Yue Depeng[1] Di Yang[2] Zhang Qibin[1] Ma Huan[1] Li Yutong[3]

(1. *Beijing Key Laboratory of Precision Forestry*, *Beijing Forestry University*, *Beijing* 100083, *China*
2. *Department of Geography University of Florida*, *Gainesville FL* 32611, *USA*
3. *Center for Land Consolidation*, *Ministry of Land and Resources*, *Beijing* 100035, *China*)

Abstract: In the ecologically vulnerable area which locates in northwest arid and semiarid areas, ecological land is the important guarantee to maintain the security and stability of regional ecological environment. Studying the simulation of ecological land use change is of great significance. Accordingly, based on the typical ecologically vulnerable area—Dengkou County, this paper simulates ecological land use evolution of Dengkou County, using the four remote sensing image interpretation data of 2002, 2007, 2012 and 2015. Taking ecological eco-resistance barriers and EnKF – MCRP model into account, an ecological resistance surface was built. The EnKF – MCRP model was constructed to simulate the evolution of ecological sources considering the ecological sources change, ecological source level, distance and base surface resistance characteristics. The results showed that the combination of data assimilation and EnKF – CA/Markov model made a total accuracy of 82.4%, by using ensemble Kalman filter, the model can accumulate less errors and improve the accuracy of simulation, i. e., data assimilation can reduce the accumulation of errors. According to the expandability, ecological sources of Dengkou County were divided into five grades, of which the spatial layout of 3, 4, 5 grades formed the northeast-southwest and northwest-southwest pattern of desertification prevention. The building of EnKF – MCRP which takes the ecological source evolution into consideration made the highest precision. And the area of ecological sources and spatial distribution were the closest to the reality, of which the variance met 0.4. Different levels of ecological sources and ecological barriers were used to modify the model, which can improve the accuracy of the simulation results. This study could provide a scientific basis for the current and future ecological land planning and management.

Key words: ecological land; data assimilation; EnKF – MCRP model; Dengkou County

0 Introduction

Ecological land has important ecosystem services, high sensitivity and fragile ecological environment. It is a land unit which can maintain the important role of regional key ecological processes[1]. In the northwest desert oasis transition region, the ecosystem is extremely fragile. Ecological land is a "buffer"[2], it can accelerate the prevention and mitigation of land desertification expansion. It also has multiple functions, such as maintaining the healthy and sustainable development of the oasis ecosystem, providing the ecosystem services and so on. Therefore, the simulation of ecological land use change in the ecological fragile area of the desert oasis has become a hot spot of the scholars around the world. The reconstruction, simulation and prediction of ecological land can provide effective demonstration and support for the rational utilization, scientific planning and improvement of the ecological land resources in the desert oasis area.

Minimum cumulative resistance model is widely used in the field of species conservation and landscape pattern analysis[3-4]. MCR model was used by many scholars to study the land use planning, urban land expansion simulation, ecological protection land expansion trend analysis, urban land ecological suitability evaluation, mountain urban growth boundary

Received date: 2016 – 06 – 16 Accepted date: 2016 – 06 – 30
Supported by National Natural Science Foundation of China (Grant No. 41371189), "Twelfth Five-year" National Key Technology Support Program (Grant No. 2012BAD16B00)
Corresponding author: Yue Depeng, Professor. E-mail: yuedepeng@126.com. Tel: +86 – 137 – 18876897.

delimitation and so on[5-6]. In the construction of the ecological resistance model, the source, distance and resistance of the three factors are considered in most of the studies, and the study on the source level is relatively less in the construction of resistance model[7]. There is no research on changes in the ecological source. The source of ecological land is of great significance. It changes with the time and the external conditions. Data assimilation can assimilate the observed data from different sources to modify the dynamic process model. At present, different data assimilation algorithms have been used by many scholars in urban expansion simulation[8], land use simulation[9], land surface system simulation[10] and so on. These studies show that the data assimilation can update the model and improve the accuracy of the model[8]. Data assimilation techniques, the research hotspot at present, are introduced to the ecological source change simulation[11]. Assimilation value is used to improve source change simulation results, and the change of source is introduced into the ecological resistance surface model. In addition, ecological source expansion capacity factor is used to modify MCR model. In this paper, the ecological resistance model suitable for the desert oasis area is constructed.

In this paper, Dengkou County, a typical city in desert oasis area, is selected as the research area. The EnKF algorithm is used for simulation and correction of ecological source changes, to construct ecological resistance model. This model includes four elements: ecological sources change, source level, distance and ecological resistance/disorder. Then, the ecological land use expansion in Dengkou County was simulated.

1 Materials and methods

1.1 General situation of study area

Dengkou County is located in northwestern of China. The coordinate of this area is 107°05′ E and 40°13′ N. Dengkou County locates in the terrain surrounded by the Inner Mongolia Hetao Plain, backed by the Langshan Mountain, and locates in northeast of Ulan Buh Desert. The altitude is 1 030 ~ 2 046 m in Dengkou County, and the altitude in the southeast is higher than that in the northwestern, except for the mountainous area. The climate of the area is temperate continental monsoon, for example, the average wind speed is 3.0 m/s, instantaneous maximum wind speed is 28 m/s, average annual rainfall is 143.9 mm, average annual potential evaporation is 2 327 mm, average temperature is 7.6℃, and frost free period is 136 days. Otherwise, 6 soil classes, 10 sub classes, 31 soil genera and 258 soil types can be found in this area. The total length of Dengkou County going through the Yellow River is 52 km and annual runoff that covers 36,100 acres is 31 billion m^3. The depth of He Tao area groundwater is 0.5 ~ 3 m, the depth of sandy area groundwater is 3 ~ 10 m, and the depth for alluvial soil groundwater in front of the mountain is 3 ~ 30 m. Abundant surface water and groundwater strongly support the development of Dengkou County and the expansion of ecological land.

1.2 Data sources and processing

Landsat TM images (2000, 2007 and 2012) and Landsat OLI image (2015) with few cloud were selected as main research material in this article, the resolution of both images is 30 m. At the same time, vegetation map in 2012 (1:50 000), land use map in 2015 (1 : 50 000), and Digital Elevation Model (DEM, 30 m) were used as secondary data. By using ENVI 5.1 software, we carried out the synthesis of the image, as well as image enhancement, and geometric correction were also conducted in this research. Maximum likelihood supervised classification method was chosen to be the visual interpretation for remote sensing image for four stages[12], to extracted the ecological land information, and it is the basic ecological land. It has an irreplaceable important role in improving the environment, maintaining regional ecological balance, including lakes, beaches, reservoirs, ponds, waters and the natural desert shrub forest, artificial green space, forest and grassland. ArcMap 10.2 was used to deal with fine plaque, and superposition analysis was used for spatial data analysis. Finally, this research made use of ArcInfo 10.2 to manage the topology image and correction processes.

1.3 Technology roadmap

Using the constructed EnKF - MCRP model to simulate the ecological land expansion in Dengkou County, the overall technical route is shown in Fig. 1.

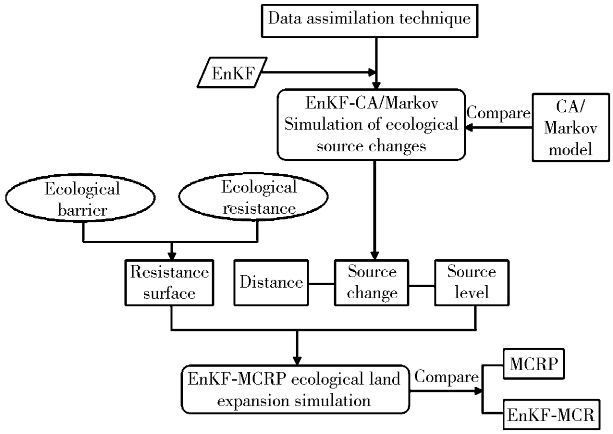

Fig. 1 Technical roadmap

1.4 Analog source change based on EnKF

The types of ecological land in Dengkou County include artificial ecological land and natural ecological land. The wetland ecological land and desert vegetation ecological land can be used as the ecological sources[2]. Ecological source is continuously changing with time, and this change can affect the regional ecological land pattern. Ensemble Kalman filter (EnKF) algorithm, one of the data assimilation method, was used for simulation of source changes, and the CA/Markov model was used as model operator, then the source changes were introduced to the ecological land expansion simulation[13].

1.4.1 Ensemble Kalman filter

Ensemble Kalman filter model regards state prediction as approximate random dynamic prediction. A state population (assuming the number of N, representing the set number) was used to represent the probability density function of the stochastic dynamic prediction[14]. The general probability density function of the next moment state was calculated by forward integration, and the statistical properties (such as mean and covariance) of the time are obtained[15-16].

The calculation steps of the set Kalman filtering algorithm are as follows:

(1) Initialize ensemble of model states.

$$\boldsymbol{X}_k = (\boldsymbol{X}_k^1, \boldsymbol{X}_k^2, \cdots, \boldsymbol{X}_k^N) \quad (\boldsymbol{X}_k \in \mathbf{R}^{n \times N}) \tag{1}$$

where n is the number of model states variables, N is the size of ensemble and k is the time.

(2) Calculate the forecasted variable of model states $\boldsymbol{X}_{k+1}^f$ at time $k+1$.

$$\boldsymbol{X}_{k+1}^f = M(\boldsymbol{X}_k^a) + \boldsymbol{\omega}_k \quad (\boldsymbol{\omega}_k \sim N(0, \boldsymbol{W}_k)) \tag{2}$$

where $\boldsymbol{X}_{k+1}^f$ is the forecasted variable of model states at time $k+1$. $\boldsymbol{X}_k^a$ is the analyzed variable of model states at time k. $\boldsymbol{\omega}_k$ is model error vector, which conforms to Gaussian distribution with zero mean and covariance matrix $\boldsymbol{W}_k$. $M(\,)$ is the CA/Markov model in this paper. The source of change can be seen as Markov[17] in the study of source change simulation. For example, in this paper, using the source data in 2002 and 2007, the spatial distribution of source in 2012 could be predicted. And then compared with the actual source data in 2012, the source of plaque in 2007 may correspond to the Markov process, it is only associated with the source patch in 2002. Different levels of source conversion area number or proportion is the state transition probability[18-19].

(3) Calculate the Kalman gain matrix $\boldsymbol{K}_{k+1}$ at time $k+1$.

$$\boldsymbol{K}_{k+1} = \boldsymbol{P}_{k+1}^f \boldsymbol{H}^{\mathrm{T}} (\boldsymbol{H}\boldsymbol{P}_{k+1}^f \boldsymbol{H}^{\mathrm{T}} + \boldsymbol{R})^{-1} \tag{3}$$

where,

$$\boldsymbol{P}_{k+1}^f = \frac{1}{N-1} \sum_{i=1}^{N} (\boldsymbol{X}_{k+1}^f - \overline{\boldsymbol{X}}_{k+1}^f)(\boldsymbol{X}_{k+1}^f - \overline{\boldsymbol{X}}_{k+1}^f)^{\mathrm{T}}$$

$$\overline{\boldsymbol{X}}_{k+1}^f = \frac{1}{N} \sum_{i=1}^{N} \boldsymbol{X}_{k+1}^{f_i}$$

$$\boldsymbol{P}_{k+1}^f \boldsymbol{H}^{\mathrm{T}} = \frac{1}{N-1} \sum_{i=1}^{N} (\boldsymbol{X}_{k+1}^f - \overline{\boldsymbol{X}}_{k+1}^f)(\boldsymbol{H}(\boldsymbol{X}_{k+1}^f) - \boldsymbol{H}(\overline{\boldsymbol{X}}_{k+1}^f))^{\mathrm{T}}$$

$$\boldsymbol{H}\boldsymbol{P}_{k+1}^f \boldsymbol{H}^{\mathrm{T}} = \frac{1}{N-1} \sum_{i=1}^{N} (\boldsymbol{H}(\boldsymbol{X}_{k+1}^f) - \boldsymbol{H}(\overline{\boldsymbol{X}}_{k+1}^f)) \cdot (\boldsymbol{H}(\boldsymbol{X}_{k+1}^f) - \boldsymbol{H}(\overline{\boldsymbol{X}}_{k+1}^f))^{\mathrm{T}}$$

where $\boldsymbol{P}_{k+1}^f$ is the forecasted background error covariance matrix. $\boldsymbol{H}$ is observation operator. $\boldsymbol{R}$ is observation error covariance. $\overline{\boldsymbol{X}}_{k+1}^f$ is the forecasted state variable mean of ensemble members.

(4) Calculate the analyzed variable of model states $\boldsymbol{X}_{k+1}^a$ and the analyzed error covariance matrix $\boldsymbol{P}_{k+1}^a$.

$$\boldsymbol{X}_{k+1}^a = \boldsymbol{X}_{k+1}^f + \boldsymbol{K}_{k+1}[(\boldsymbol{Y}_{k+1} + \boldsymbol{\nu}_{k+1}) - \boldsymbol{H}(\boldsymbol{X}_{k+1}^f)] \quad (\boldsymbol{\nu}_{k+1} \sim N(0, R)) \tag{4}$$

$$\boldsymbol{P}_{k+1}^a = \frac{1}{N-1} \sum_{i=1}^{N} (\boldsymbol{X}_{k+1}^a - \overline{\boldsymbol{X}}_{k+1}^a)(\boldsymbol{X}_{k+1}^a - \overline{\boldsymbol{X}}_{k+1}^a)^{\mathrm{T}} \tag{5}$$

where,

$$\overline{\boldsymbol{X}}_{k+1}^a = \frac{1}{N} \sum_{i=1}^{N} \boldsymbol{X}_{k+1}^{ai} \tag{6}$$

where $\boldsymbol{Y}_{k+1}$ is the observation at time $k+1$. $\boldsymbol{\nu}_{k+1}$ is random error vector of observation with zero mean and covariance matrix $\boldsymbol{R}$.

(5) If it is the end stage of assimilation, end the program. Else, back to step (2).

1.4.2 Implementation of EnKF and CA/Markov model

Data assimilation offers the advantage to integrate various amounts of observations and model predictions for improved estimates of states. It requires that the input data is non boolean. While the CA/Markov model which simulate is the result state of cell only has two species, i. e., the source and non-source[13-20]. Therefore, it is necessary to make some adjustments. In this paper, the study area is divided into grids. Each grid contains a certain number of pixels (cells).

The calculation formula of cell expansion strength is as follows:

$$\Omega_{ij}^{t} = \frac{\sum_{m \times m} con(s_{ij} = source)}{mm} \tag{7}$$

where the number of cells inside a grid is $m \times m$. $con(s_{ij} = source)$ is the number of endogenous cells in the region.

Using the above equation, each grid has a developing density of continuous numerical value. We assume that each member of ensemble in $\boldsymbol{X}_k^f$ is correspond to a developing density of a grid. The analysis value $\boldsymbol{X}_{k+1}^a$ can be derived by use of Eq. (4). The simulation results of CA model can be updated based on the derived analysis value. The CA model based on ensemble Kalman filter was established. The steps of model establishment are detailed as follows: ① derive the developing density of each grid $\boldsymbol{X}_k^f$ from the simulated results of CA model at assimilation time. ② obtain the analysis values $\boldsymbol{X}_{k+1}^a$ by Eq. (4) after setting the parameter values of EnKF. ③ update the simulated results based on analysis values $\boldsymbol{X}_{k+1}^a$.

Using the Fishnet module of ArcGIS software, the whole area was divided into 513 regular blocks, and 66 observation points and 56 detection points (Fig. 2) were selected.

For statistical error, variance (SE) was adopted and calculated as follow:

$$V_{SE} = \sum_{i=1}^{N} (y_i - x_i)^2 \tag{8}$$

where y is true value, x is assimilated values or simulated values. y has the same number of dimensions as x.

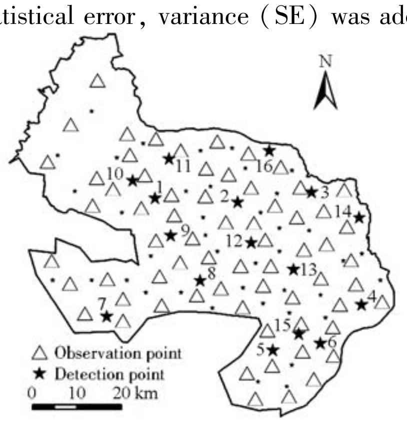

Fig. 2 Spatial distribution of observation points and detection points

1.5 MCRP model

Ecological land expansion can be regarded as a competitive control process of ecological green space to other land use space. And this control and coverage must overcome the resistance[5, 21-22]. This extension can be seen as a horizontal process from source to sink[23]. The basic formula of MCR model is:

$$V_{\text{MCR}} = f_{\min} \sum_{j=n}^{i=m} D_{ij} R_i \tag{9}$$

where $f_{\min}$ is a function of the positive correlation that reflects the relation of the least resistance for any point in space to the distance from any point to any source and the characteristics of the landscape base surface; min denotes the minimum value of cumulative resistance produced in different processes of landscape unit i transforming into a different source unit j; D_{ij} is the spatial distance between landscape unit i and source unit j; and R_i denotes the resistance coefficient that exists in transition from landscape unit i to source unit j.

Different ecological sources have different ecological expansion ability. Different levels of ecological source expansion ability factor P_j was introduced to modify MCR model. In order to simplify the calculation, ecological source patch area value was used to classify ecological sources. And using ArcGIS 10.2 software to give the value of the expansion ability.

The EnKF - CA/Markov model was used to predict the ecological sources in 2017. This prediction result was used for data assimilation with ecological sources in 2012. The spatial distribution of ecological source assimilation contains ecological source information in 2012, also includes the future trend of the ecological source.

The ecological model of resistance source expansion capacity constraints is constructed, i. e., MCRP model (Minimal cumulative resistance power). The modified model is composed of four factors, including the sources, the source level, the distance and the base resistance characteristics. The modified formula is expressed as:

$$V_{\mathrm{MCR}}P = f_{\min}\sum_{j=n}^{i=m} D_{ij}R_iP_j \qquad (10)$$

where P_j indicates the relative energy factor of the source j, the higher the value of P_j, the greater the energy of the ecological source.

2 Results and analysis

2.1 Simulation source change and classification

According to the image interpretation data of 2002, 2007 and 2012, combined with the actual situation of Dengkou County, ecological sources were extracted. In the desert oasis region, the ecological function of wetland is huge, so all the waters were extracted as ecological source. In Dengkou County, the windbreak function of desert shrub land is significant, ecological function is very important, the area more than 0.1 km^2 of the desert shrub land was extracted as a source.

EnKF algorithm was used to simulate the spatial-temporal evolution of source. And the CA/Markov model was used as the operator of data assimilation. The size of the collection was set to 30, data assimilation operator parameters included distance factor, terrain factor, and hydrological factor. As shown in Fig. 3.

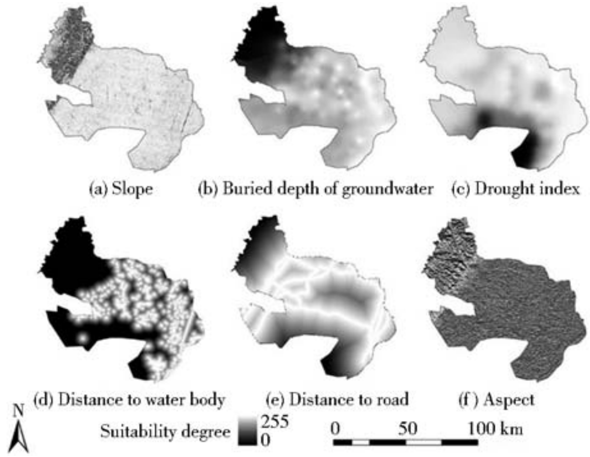

Fig. 3 Evaluation of various types of suitability factors

Using CA/Markov model and EnKF – CA/Markov model, based on the source data in 2002 and 2007, forecasted the source spatial distribution in 2012 (Figs. 4b and 4c), and compared it with the actual situation of ecological land (Fig. 4a).

IDRISI software was used to carry out pixel by pixel comparison analysis, the total accuracy of EnKF – CA/Markov model simulation is 82.4%, the simulation results variance is 0.6, and Kappa coefficient is 0.513. The simulation precision of the traditional CA/Markov model is 65.4%, the variance of simulation results is 1.3, and the Kappa coefficient is 0.342. In the process of simulation, the simulation results were improved by using the data assimilation technique. In this study, the model can reduce the accumulation of errors and improve the accuracy of simulation by introducing the Ensemble Kalman filter.

Based on the source data in 2007 and 2012, EnKF – CA/Markov was used to predict the spatial distribution of the source in 2017. Source spatial distribution in 2017 is shown in Fig. 5a. Ecological source in 2017 was used as the estimated value of EnKF model, the actual ecological sources in 2012 and ecological source in 2017 were used for data assimilation. Ecological source assimilation data in 2017 and 2012 were obtained (Fig. 5b), which includes both the ecological source information in 2012, and the trend of ecological land use change to 2017.

According to the source of capacity expansion, the source level was divided. The total is divided into five levels (Fig. 5c), the higher level represents the source expansion ability is stronger. Level 5 source distribution in Dengkou County outside of Baulerhaute Gacha, Bayanondor Gacha, Ondormaodao Gacha and Wulanbuhe farm land, from southwest to northeast

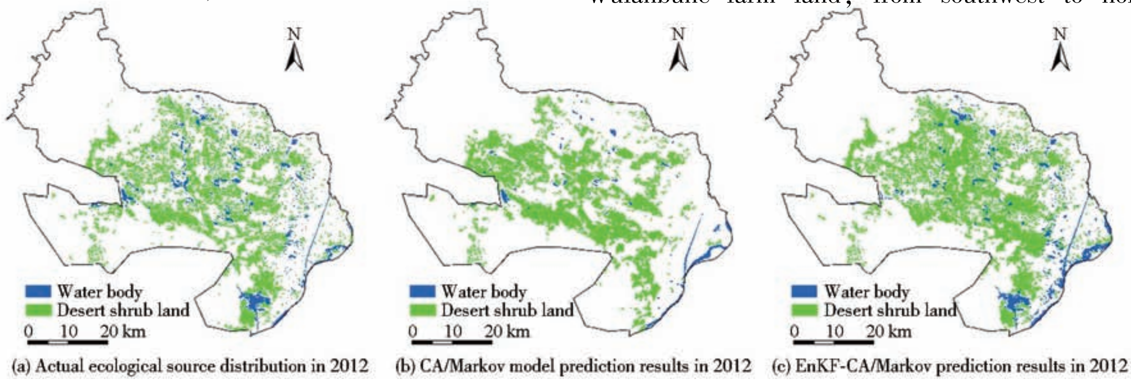

Fig. 4 Actual and model simulated spatial distribution map of ecological source in 2012

through Dengkou County, connects with Nailun Lake. The level 4 ecological source is mainly distributed on the periphery of Bayingarina Gacha, Hatengtaohai farmland and Nalintaohai farmland. Level 3 ecological source is mainly distributed in Dengkou County near the sand forest, Nailun Lake, Baoergai farm. 3, 4, 5 ecological sources constitute the northwest-southwest and northeast-southwest desert protection pattern. This pattern can prevent and control the expansion of the Ulan Buh desert.

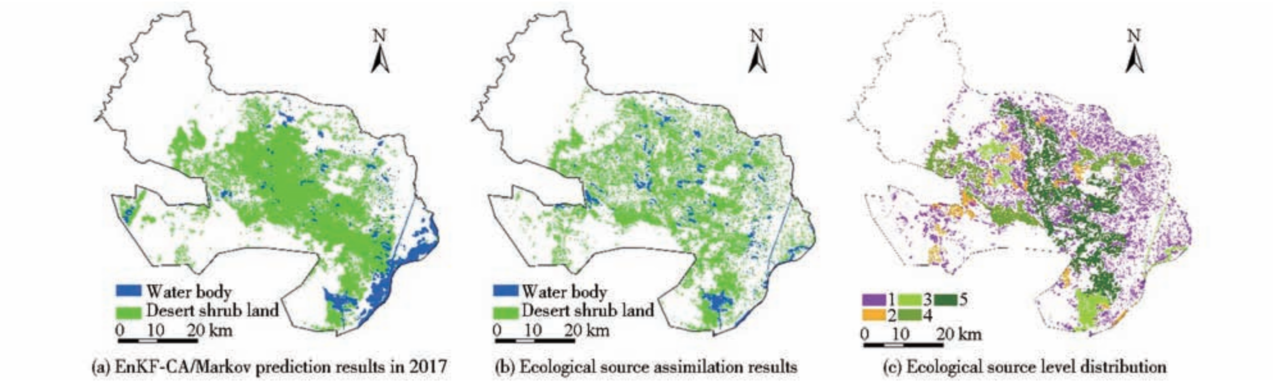

Fig. 5 Distribution map of ecological sources and classification of space

2.2 Construction of ecological resistance surface

Due to differences in the surface characteristics, ecological land resistance in the process of expansion is different, the resistance coefficient reflects the degree of difficulty that ecological land control and cover other land use types. The surface resistance was divided into two categories: ecological barriers and ecological resistance. Ecological barrier is the land cannot be extended to the ecological land, such as construction land, basic farmland and so on, constitute the rigid constraints of the expansion of ecological land, the resistance coefficient is infinite. Ecological resistance is a land mass which has different effects on the expansion of ecological land. Considering the inherent attributes and additional attributes of the land surface, the evaluation system of ecological resistance was constructed. The ecological resistance was divided into five levels, level 1 indicates the minimum resistance, level 5 indicates the maximum resistance. Intrinsic attributes include land type and geological features. Additional attributes include ecosystem services value and NDVI- water body distance. The constructed resistance evaluation system is shown in Tab. 1 and Tab. 2.

Tab. 1 Evaluation system of ecological resistance

Project	Attribute value				
	1	2	3	4	5
Land type	Natural lakes, ponds, rivers and ditches, reservoirs etc.	Desert shrub, urban green land, natural grass land, etc.	Cultivated land	Urban and construction land	Desert
Topographic features	Extremely soft matrix	Low soft substrate	Soft matrix	Low hard substrate	Hard substrate
Service function	Water supply, flood control, drainage, water purification, carbon dioxide absorption, and oxygen release	Wind, prevent desertification, wildlife habitat	Maintenance of biological diversity, biomass production	To provide land for human habitation	Non

Tab. 2 Evaluation system of ecological resistance between NDVI and water distance

NDVI	The distance between it and the water body/km				
	0 ~ 30	30 ~ 60	60 ~ 120	120 ~ 180	> 180
0.8 ~ 1.0	1	1	2	2	2
0.6 ~ 0.8	1	2	2	3	3
0.4 ~ 0.6	2	3	3	4	4
0.2 ~ 0.4	2	3	4	4	4
0 ~ 0.2	3	4	5	5	5

First of all, the ecological land space expansion barriers were identified. The first category is the basic farmland, it can guarantee the regional economic and social stability in Dengkou County, and its area is 796.28 km^2. The second category is construction land, it is the rigid limit of ecological land expansion. The distribution map of ecological barrier is shown in Fig. 6a.

Then, the ecological resistance surface was determined according to the evaluation system of ecological resistance. According to the MCRP model, using cost-distance module of ArcGIS software, ecological source surfaces of ecological source of five levels were separately generated. The superposition operation was carried out to generate the resistance surface of ecological land expansion, as shown in Fig. 6b. The minimum cumulative resistance value is 0, which is located in the interior of the ecological land. The maximum cumulative resistance value is 77 780. 8, located inside the Ulanbuh Desert. According to the accumulated resistance surface, the resistance of the outer of ecological land is larger, and the obvious "ridge line" is formed. This phenomenon is due to the large area of desert in the periphery of the desert shrub land. The area with low accumulation resistance is broken and the integrity is poor, which seriously affects the flow of landscape flow. The ecological environment in arid area is fragile, and the serious desertification leads to the poor flow of landscape ecology. The inherent attribute leads to the large resistance of landscape flow. However, the increase of the artificial impervious surface caused by urbanization, which further aggravated the landscape fragmentation and increased the flow resistance of the landscape.

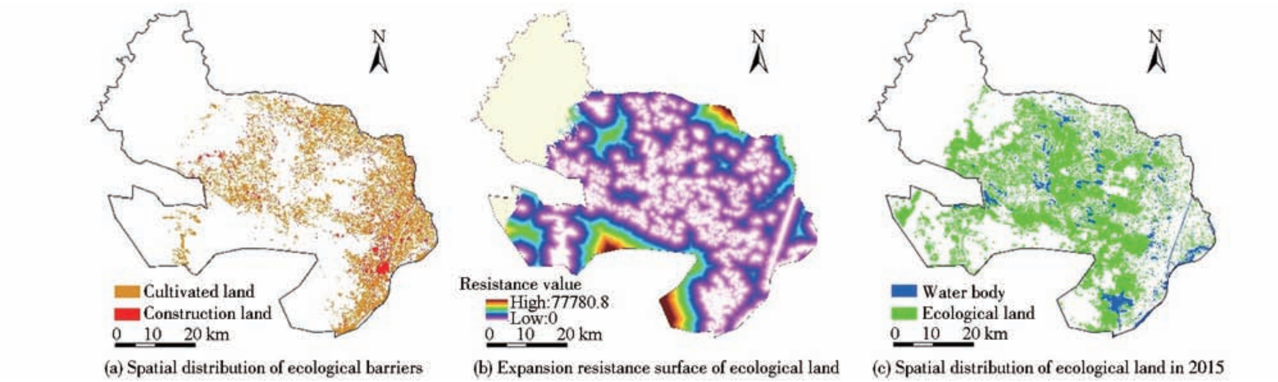

Fig. 6 Ecological barrier, resistance surface and spatial distribution of ecological land in 2015

2.3 Ecological land expansion simulation

Python scripting language was used to prepare the program to simulate the model in the ArcGIS 10.2 software. The data in 2012 was selected as the data base, the time threshold was set to 3 a. Based on the generated resistance surface, the actual data of ecological source in 2012 and the assimilation data of ecological source, the MCR model and the MCRP model were used to simulate the ecological land expansion, and to simulate the ecological land use in 2015 respectively (Fig. 6c). In order to facilitate the validation, the ecological land area in 2015 was used as the test standard. Wetland ecological land area is 137. 92 km^2 in Dengkou County in 2015. The total area of desert vegetation type, natural oasis type, and urban oasis type and wasteland type ecological land is 1 042. 96 km^2.

After the iterative calculation, EnKF - MCRP model simulation of the ecological land area is 1 260. 95 km^2 (Fig. 7a), MCRP model simulation of the ecological land area is 983. 57 km^2 (Fig. 7b), EnKF - MCR model simulation of the ecological land area is 1 631. 35 km^2 (Fig. 7c). Compared with the actual ecological land area in 2015, MCRP simulation model

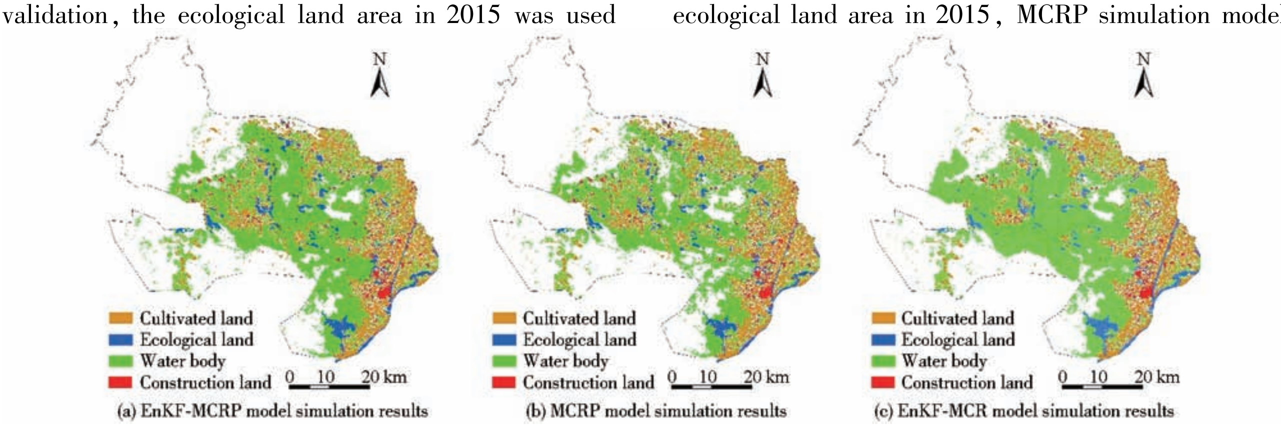

Fig. 7 Spatial distribution map of ecological land use through model simulation

which multi period changes of ecological sources and data assimilation technique are considered has the highest accuracy. Its pixel by pixel variance is 0.4, and the overall ecological land space layout is close to the actual situation, the simulation accuracy of the MCRP model is followed, the variance is 1.7. Because of changes in ecological sources are considered, the area of MCRP model simulation is slightly larger than that of ecological land in 2015. MCRP model simulation results without the use of data assimilation techniques are smaller than the actual. This phenomenon shows that the data assimilation technology can improve the accuracy of the model simulation. The change of ecological sources as a model of factors is necessary. Compared with the EnKF – MCRP model, the simulation results of the EnKF – MCR model is lower, its pixel by pixel variance is 3.1, and its simulation results are much more than the true value of 450.37 km^2. This result shows that when constructing ecological resistance surface, the source of different grades of ecological resistance should be considered. In addition, the rigidity of the ecological barrier limits should be considered. From the simulation results, the simulation results of the ecological land expansion without considering the ecological barrier obviously occupied the basic farmland and construction land.

The land use types and the actual land use types of the 56 detection points were compared and verified. Among them, the consistent assignment is 1, the inconsistent assignment is 2. Consistency comparison showed that the simulation results of EnKF – MCRP model are more consistent with the actual situation. In the simulation results of MCRP model, 11 points are not consistent with the actual results, and 19 points in EnKF – MCR simulation results are not consistent with the actual results.

16 representative detection points are selected from 56 detection points and the simulation results are analyzed (Tab. 3). At the detection points 1, 3, 4, 5, 6, 11, 14, 15 and 16, the simulation results of EnKF – MCRP, MCRP and EnKF – MCR model are in accord with the reality. The role of assimilation is obvious, especially the detection point 2. In 2015, the detection point 2 is ecological land. The simulation results of EnKF – MCRP and EnKF – MCR model are consistent with the actual results, but the MCRP model simulation results are not consistent with the actual results. This results show that the data assimilation has a significant effect on the improvement of simulation accuracy. Detection points 12, 10 are located in the edge of ecological land. The model simulation results based on the data assimilation technique are in accord with the practice, and the MCRP model simulation results without the use of the data assimilation technique are relatively low. If the iteration of the year changes may lead to inaccurate simulation results. In general, all points in the assimilation process can get the correct gain information from the observation point. So it can get a better error correlation matrix, which can be used in the gain matrix to get better assimilation value. The data assimilation technique can combine the information of the observation point. The assimilation value is closer than the simulation value to the true value. Therefore, the data assimilation method is introduced into the model, which can obtain better simulation results. Detection points 7, 8 and 9 are in the ecological barrier, the detection point 13 is located on the edge of the ecological barrier, and the simulation results of EnKF – MCRP and MCRP model are in agreement with the actual results. In contrast,

Tab. 3 Land type for some detection points

Detection point	EnKF – MCRP	MCRP	EnKF – MCR	The actual situation in 2015	Position
1	1	1	1	1	Inside
2	1	4	1	1	Inside
3	1	1	1	1	Edge
4	2	2	2	2	Inside
5	3	3	3	3	Inside
6	2	2	2	2	Inside
7	2	2	1	2	Edge
8	2	2	1	2	Edge
9	2	2	1	2	Edge
10	1	1	1	1	Edge
11	3	3	3	3	Inside
12	1	1	1	1	Inside
13	2	2	2	2	Edge
14	2	2	2	2	Inside
15	1	1	1	1	Inside
16	1	1	1	1	Edge

Note: 1 represents the ecological land, 2 represents the ecological barrier, 3 represents the desert, and 4 represents the non-ecological land.

the simulation result of EnKF – MCR model is ecological land. This difference indicates an excessive expansion of ecological land. It is necessary to consider the ecological barrier in the construction of the ecological resistance surface model.

3 Conclusions

(1) In Dengkou County, ecological sources included wetlands ecological land and desert vegetation ecological land. It played an important role in maintaining the stability and development of regional ecological land. Simulation of changes of ecological source and data assimilation technique was applied in this paper. This application can quantify the change trend of the ecological source. The simulation accuracy of the EnKF – CA/Markov model was 82.4%, which can reduce the accumulation of errors and improve the accuracy of simulation by the introduction of Ensemble Kalman filter.

(2) According to the ability of ecological source, ecological source of Dengkou County was divided into five grades. Research showed that: level 3, 4 and 5 ecological source spatial layout was from northeast to southwest and northwest to southwest desert protection pattern in Dengkou County. This pattern had important significance for the prevention and treatment of Ulanbuh Desert expansion, and it played a significant role in maintaining the stability of regional ecological environment.

(3) Ecological resistance and resistance were considered in the construction of ecological resistance surface. In the construction of resistance surface, the ecological barrier was introduced, which can prevent the excessive expansion of the ecological land. Ecological sources change, ecological source level, distance and base resistance were used to construct the MCRP model. The minimum cumulative resistance value was 0, the maximum was 77 780.8, and the resistance of the ecological barrier was infinite. The results showed that the simulation accuracy of the EnKF – MCRP model was the highest. The ecological land area and space layout were close to the actual situation, and the effect of data assimilation on the simulation accuracy was obvious.

References

[1] ZHOU Rui, WANG Xinjun, SU Hailong, et al. Identification and security pattern of ecological land in Pingdingshan newly developed area[J]. Acta Ecologica Sinica, 2015, 35(6): 2003 – 2012. (in Chinese)

[2] ZHANG Hongqi, WANG Lixin, JIA Baoquan. A conception of ecological land use and its function classification in arid area in Northwest China [J]. Chinese Journal of Eco-Agriculture, 2004, 12(2): 5 – 8. (in Chinese)

[3] YUE Depeng, WANG Jiping, LIU Yongbing, et al. Spatial and temporal characteristics of agricultural land-use and landscape pattern changes in northwest of Beijing [J]. Transactions of the CSAE, 2008, 24(6): 89 – 95. (in Chinese)

[4] LIANG Man, SUN Xuan, YANG Zhen. Evaluation on spatial accessibility of ecological circulation of landscape—a case of Jingzhou City[J]. Henan Science, 2014, 32(8): 1654 – 1658. (in Chinese)

[5] YE Yuyao, SU Yongxian, ZHANG Hong'ou, et al. Ecological resistance surface model and its application in urban expansion simulations [J]. Acta Geographica Sinica, 2014, 69(4): 485 – 496. (in Chinese)

[6] YU Q, YUE D P, WANG J P, et al. The optimization of urban ecological infrastructure network based on the changes of county landscape patterns: a typical case study of ecological fragile zone located at Deng Kou (Inner Mongolia)[J]. Journal of Cleaner Production, doi: 10.1016/j.jclepro.2016.05.014.

[7] LI F, Ye Y P, SONG B W. Evaluation of urban suitable ecological land based on the minimum cumulative resistance model: a case study from Changzhou, China [J]. Ecological Modelling, 2015, 318: 194 – 203.

[8] ZHANG Yihan, LI Xia, LIU Xiaoping, et al. The CA model based on data assimilation[J]. Journal of Remote Sensing, 2011, 15(3): 475 – 491. (in Chinese)

[9] GUI Yufeng, JI Yuan, YANG Hui. The research of urban sprawl with the stochastic cellular automata model based on particle filter[J]. Mathematics in Practice and Theory, 2015, 45(17): 222 – 227. (in Chinese)

[10] ZHANG Shenglei, CHEN Liangfu, SU Lin, et al. A data assimilation-based method for optimizing parameterization schemes in a land surface process model[J]. Science China: Earth Sciences, 2015, 45(12): 1907 – 1922. (in Chinese)

[11] HUANG Jianxi, LI Xinlu, LIU Diyou, et al. Comparison of winter wheat yield estimation by sequential assimilation of three different spatial-temporal resolution remotely sensed LAI datasets[J]. Transactions of the Chinese Society for Agricultural Machinery, 2015, 46(1): 240 – 248. (in Chinese)

[12] LI Baojie. Study on landscape pattern changes and ecological effects in mining area—A case study in Jiawang mining area [D]. Xuzhou: China University of Mining and Technology, 2014. (in Chinese)

[13] ZHANG Yihan, QIAO Jigang, AI Bin. Parameter optimization for CA model using ensemble Kalman filter [J]. Acta Geodaetica et Cartographica Sinica, 2013, 42(1): 123 - 130. (in Chinese)

[14] WANG Wen, LIU Yongwei, KOU Xiaohua, et al. EnKF and HYDRUS - 1D based data assimilation experiments for improving soil moisture profile prediction [J]. Journal of Hydraulic Engineering, 2012, 43(11): 1302 - 1311. (in Chinese)

[15] LI Yuan. Chlorophyll a concentration remote evaluation in Lake Taihu based on data assimilation [D]. Nanjing: Nanjing Normal University, 2014. (in Chinese)

[16] GAO Binbin. Application research on the ensemble Kalman filter (EnKF) with a medium-range numerical weather prediction (NWP) spectral model at a T106L19 resolution [D]. Nanjing: Nanjing University of Information Science & Technology, 2008. (in Chinese)

[17] HALMY M W, GESSLER P E, HICKE J A, et al. Land use/land cover change detection and prediction in the north-western coastal desert of Egypt using Markov-CA [J]. Applied Geography, 2015, 63: 101 - 112.

[18] ZHANG Ying, DING Jianli. Study on forecasting and regulation of future trend of oasis land use [J]. Journal of Arid Land Resources and Environment, 2006, 20(6): 29 - 35. (in Chinese)

[19] WANG Yousheng, YU Xinxiao, HE Kangning, et al. Dynamic simulation of land use change in Ji He watershed based on CA - Markov model [J]. Transactions of the CSAE, 2011, 27(12): 330 - 336. (in Chinese)

[20] ZHAO Dongling, DU Meng, YANG Jianyu, et al. Simulation and forecast study of land use change based on CA - Markov model [J]. Transactions of the Chinese Society for Agricultural Machinery, 2016, 47(3): 278 - 285. (in Chinese)

[21] YIN Faneng. Study of landscape ecological Planning and drainage basin ecological management in the Four-Lake basin [D]. Shanghai: East China Normal University, 2008. (in Chinese)

[22] RAY N, LEHMANN A, JOLY P. Modeling spatial distribution of amphibian populations: a GIS approach based on habitat matrix permeability [J]. Biodiversity & Conservation, 2002, 11(12): 2143 - 2165.

[23] HERZOG F, LAUSCH A, MULLER E, et al. Landscape metrics for assessment of landscape destruction and rehabilitation [J]. Environmental Management, 2001, 27(1): 91 - 107.

doi:10.6041/j.issn.1000-1298.2016.09.039

基于 EnKF－MCRP 模型的生态用地扩张模拟研究

于　强[1]　岳德鹏[1]　Di Yang[2]　张启斌[1]　马　欢[1]　李宇彤[3]

(1.北京林业大学精准林业北京市重点实验室，北京 100083；2.佛罗里达大学地理系，盖恩斯维尔 32611；
3.国土资源部土地整治中心，北京 100035)

摘要：以生态脆弱区典型县域磴口县为研究区，基于 2002、2007、2012、2015 年 4 期遥感影像解译数据，将数据同化技术引入生态源地的变化模拟中，考虑生态障碍和生态阻力构建 EnKF－MCRP 模型，进行磴口县生态用地的变化模拟。结果表明，引入数据同化技术的 EnKF－CA/Markov 模型的模拟总精度达到 82.4%，数据同化能够减少误差的积累。根据扩展能力磴口县生态源地共分为 5 个等级，其中 3、4、5 级生态源地的空间布局形成东北-西南、西北-西南的沙漠化防护格局。引入生态源地变化的 EnKF－MCRP 模型的生态用地扩张模拟精度最高，生态用地面积与空间布局最接近实际情况，方差达到 0.4。此研究可为当前以及未来的生态用地规划和管理提供科学根据。

关键词：生态用地；数据同化；EnKF－MCRP 模型；磴口县

中图分类号：K903　　**文献标识码**：A　　**文章编号**：1000-1298(2016)09-0285-09

Simulation on Ecological Land Use Expansion Based on EnKF－MCRP Model

Yu Qiang[1]　Yue Depeng[1]　Di Yang[2]　Zhang Qibin[1]　Ma Huan[1]　Li Yutong[3]

(1. *Beijing Key Laboratory of Precision Forestry*, *Beijing Forestry University*, *Beijing* 100083, *China*
2. *Department of Geography University of Florida*, *Gainesville FL* 32611, *USA*
3. *Center for Land Consolidation*, *Ministry of Land and Resources*, *Beijing* 100035, *China*)

Abstract: In the ecologically vulnerable area which locates in northwest arid and semiarid areas, ecological land is the important guarantee to maintain the security and stability of regional ecological environment. Studying the simulation of ecological land use change is of great significance. Accordingly, based on the typical ecologically vulnerable area—Dengkou County, this paper simulates ecological land use evolution of Dengkou County, using the four remote sensing image interpretation data of 2002, 2007, 2012 and 2015. Taking ecological eco-resistance barriers and EnKF－MCRP model into account, an ecological resistance surface was built. The EnKF－MCRP model was constructed to simulate the evolution of ecological sources considering the ecological sources change, ecological source level, distance and base surface resistance characteristics. The results showed that the combination of data assimilation and EnKF－CA/Markov model made a total accuracy of 82.4%, by using ensemble Kalman filter, the model can accumulate less errors and improve the accuracy of simulation, i.e., data assimilation can reduce the accumulation of errors. According to the expandability, ecological sources of Dengkou County were divided into five grades, of which the spatial layout of 3, 4, 5 grades formed the northeast-southwest and northwest-southwest pattern of desertification prevention. The building of EnKF－MCRP which takes the ecological source evolution into consideration made the highest precision. And the area of ecological sources and spatial distribution were the closest to the reality, of which the variance met

收稿日期：2016－06－16　修回日期：2016－06－30

基金项目：国家自然科学基金项目(41371189)和"十二五"国家科技支撑计划项目(2012BAD16B00)

作者简介：于强(1987—)，男，博士生，主要从事 3S 技术在生态环境中的应用研究，E-mail：yuqiang@bjfu.edu.cn

通信作者：岳德鹏(1963—)，男，教授，博士生导师，主要从事景观生态学和土地评价研究，E-mail：yuedepeng@126.com

0.4. Different levels of ecological sources and ecological barriers were used to modify the model, which can improve the accuracy of the simulation results. This study could provide a scientific basis for the current and future ecological land planning and management.

Key words: ecological land; data assimilation; EnKF－MCRP model; Dengkou County

引言

生态用地是具有重要的生态系统服务功能或生态敏感性较高、生态环境较为脆弱、对维护区域关键生态过程发挥重要作用的土地单元[1]。在西北荒漠绿洲过渡区，覆盖区域的生态系统极其脆弱，生态用地作为干旱区防治和减缓土地荒漠化加速扩展的“缓冲剂”[2]，还具有维护绿洲生态系统健康和持续发展、提供生态服务等多重功能，因此荒漠绿洲生态脆弱区生态用地变化模拟已成为全世界学者们的研究热点。生态用地的重建、模拟及预测可以为荒漠绿洲区生态用地资源的合理利用、科学规划以及改善区域生态环境提供有效示范和支撑。

最小累计阻力模型（Minimal cumulative resistance，MCR）被广泛应用于物种保护和景观格局分析等生态领域[3-4]，众多学者利用MCR模型进行了旅游用地规划、城市用地扩张模拟、生态保护用地扩张趋势分析、城市土地生态适宜性评价、山区城市增长边界划定等研究[5-6]，在构建生态阻力模型时均考虑了源、距离和阻力3个因素，目前考虑源地等级研究较少，考虑源地的变化则基本没有[7]。作为源地的生态用地意义重大，其随着时间及外界条件不断发生变化，数据同化能够同化不同来源的观测数据以修正动态过程模型，目前众多学者应用不同的数据同化算法进行了城市扩张模拟[8]、土地利用模拟[9]、陆面系统模拟[10]等研究，研究表明数据同化能更新（修正）模型并提高模型的模拟精度[8]。本文将目前的研究热点数据同化技术引进到生态源地的变化模拟中[11]，利用同化值修正源地变化的模拟结果，并将源地的变化引入到生态阻力面模型中，另外考虑生态源地扩张能力因子修正MCR模型，构建适合荒漠绿洲区的生态阻力模型。

本文选择荒漠绿洲区典型城市磴口县为研究区，采用数据同化技术中的集合卡尔曼滤波算法模拟修正生态源地的变化，构建考虑源地变化、源地等级、距离、生态阻力/障碍4方面的生态阻力模型，对磴口县的生态用地扩张进行模拟。

1 材料与方法

1.1 研究区概况

磴口县地处中国西北部（东经107°05′，北纬40°13′），位于内蒙古河套平原源头，黄河中上游，背靠狼山山脉，西邻乌兰布和沙漠。磴口县气候干旱少雨，水资源较为短缺，土地沙漠化严重，土地退化严重，区域蒸发量大，导致土地盐渍化程度深，境内海拔高度1 030～2 046 m，整个地形除山区外，呈东南高西北低，逐渐倾斜。属中温带大陆性季风气候，历年平均风速3.0 m/s，瞬间最大风速28 m/s，多年平均降水143.9 mm，多年平均蒸发量2 327 mm，多年平均气温7.6℃，无霜期136 d。全县有6个土类，10个亚类，31个土属，258个土种。黄河流经磴口县52 km，年径流量3.1×10^{10} m^3，共有水域面积约24.07 km^2。河套地区地下水埋深0.5～3 m，沙区地下水埋深3～10 m，山前洪积扇地下水埋深3～30 m，相对丰富的地表水与地下水对磴口县发展以及生态用地扩张提供了有力保障。

1.2 数据来源与处理

选取磴口县夏季且少云的TM影像（2002、2007、2012年）和OLI影像（2015年）为研究对象，同时利用研究区2012年1∶5万植被分布图、2015年1∶5万土地利用图、空间分辨率30 m的DEM等作为辅助数据。利用ENVI 5.1软件对影像进行波段合成、图像增强和几何校正处理，选择最大似然监督分类法对4期遥感影像进行目视解译[12]，提取磴口县的生态用地类型信息，所提取的磴口县生态用地为基础性生态用地，其在改善环境、维持区域生态平衡方面具有不可替代的重要作用，包括湖泊、滩地、水库坑塘等水域和自然荒漠灌林地、人工绿地等林草地。使用ArcMap 10.2进行细碎斑块处理，运用叠加分析工具进行空间数据分析，最终在ArcInfo 10.2环境下完成拓扑和改错处理。

1.3 技术路线

利用所构建的EnKF－MCRP模型进行磴口县生态用地扩张模拟，总体技术路线如图1所示。

1.4 基于EnKF的源地变化模拟

磴口县的生态用地类型包括人工型生态用地和自然型生态用地，其中能作为生态源地的生态用地类型为湿地型生态用地和荒漠植被型生态用地[2]。生态源地是随着时间不断变化的，且生态源地的变化会影响区域生态用地格局。通过引入集合卡尔曼滤波的数据同化方法，使用CA/Markov模型为数据同化模型算子模拟源地的变化，并将源地变化引入

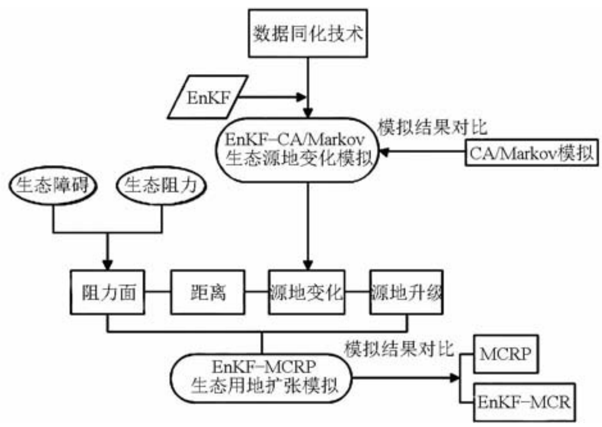

图 1　总体技术路线

Fig. 1　Technical roadmap

到生态用地扩张模拟中[13]。

1.4.1　集合卡尔曼滤波

集合卡尔曼滤波（Ensemble Kalman filter，EnKF）将模型状态预报看成近似随机动态预报，用一个状态总体（设数目为 N，即集合数）代表随机动态预报中的概率密度函数[14]，通过向前积分计算下一时刻状态总体的概率密度函数，并得到该时刻的统计特性（如均值与协方差）[15－16]。

集合卡尔曼滤波算法计算步骤如下：

（1）模型状态集合初始化为

$$\boldsymbol{X}_k = (\boldsymbol{X}_k^1, \boldsymbol{X}_k^2, \cdots, \boldsymbol{X}_k^N) \quad (\boldsymbol{X}_k \in \mathbf{R}^{n \times N}) \tag{1}$$

式中　n——模型状态变量的个数

k——时间刻度

（2）计算每个状态变量在第 $k+1$ 时刻的预报值

$$\boldsymbol{X}_{k+1}^f = M(\boldsymbol{X}_k^a) + \boldsymbol{\omega}_k \quad (\boldsymbol{\omega}_k \sim N(0, \boldsymbol{W}_k)) \tag{2}$$

式中　$\boldsymbol{X}_{k+1}^f$——第 $k+1$ 时刻的预报值，用于修正模拟结果

$\boldsymbol{X}_k^a$——k 时刻的分析值

$\boldsymbol{\omega}_k$——期望为 0、方差为 $\boldsymbol{W}_k$ 的高斯白噪声

$\boldsymbol{W}_k$——模型的误差方差矩阵

$M(\,)$为模型算子，本文指源的演变 CA/Markov 模型，在源地变化研究中，将源地变化过程看作 Markov 过程[17]，如利用 2002 年和 2007 年的源地数据预测 2012 年的源地空间分布，并与 2012 年源地实际数据进行对比，即 2007 年的源地斑块对应于 Markov 过程中的可能状态，它只与 2002 年的源地斑块状态相关，不同等级源地相互转换的面积数量或比例即为状态转移概率[18－19]。

（3）计算 $k+1$ 时刻的卡尔曼增益矩阵 $\boldsymbol{K}_{k+1}$ 为

$$\boldsymbol{K}_{k+1} = \boldsymbol{P}_{k+1}^f \boldsymbol{H}^{\mathrm{T}} (\boldsymbol{H}\boldsymbol{P}_{k+1}^f \boldsymbol{H}^{\mathrm{T}} + \boldsymbol{R})^{-1} \tag{3}$$

其中

$$\boldsymbol{P}_{k+1}^f = \frac{1}{N-1} \sum_{i=1}^{N} (\boldsymbol{X}_{k+1}^f - \overline{\boldsymbol{X}}_{k+1}^f)(\boldsymbol{X}_{k+1}^f - \overline{\boldsymbol{X}}_{k+1}^f)^{\mathrm{T}}$$

$$\overline{\boldsymbol{X}}_{k+1}^f = \frac{1}{N} \sum_{i=1}^{N} \boldsymbol{X}_{k+1}^{f_i}$$

$$\boldsymbol{P}_{k+1}^f \boldsymbol{H}^{\mathrm{T}} = \frac{1}{N-1} \sum_{i=1}^{N} (\boldsymbol{X}_{k+1}^f - \overline{\boldsymbol{X}}_{k+1}^f)(\boldsymbol{H}(\boldsymbol{X}_{k+1}^f) - \boldsymbol{H}(\overline{\boldsymbol{X}}_{k+1}^f))^{\mathrm{T}}$$

$$\boldsymbol{H}\boldsymbol{P}_{k+1}^f \boldsymbol{H}^{\mathrm{T}} = \frac{1}{N-1} \sum_{i=1}^{N} (\boldsymbol{H}(\boldsymbol{X}_{k+1}^f) - \boldsymbol{H}(\overline{\boldsymbol{X}}_{k+1}^f)) \cdot (\boldsymbol{H}(\boldsymbol{X}_{k+1}^f) - \boldsymbol{H}(\overline{\boldsymbol{X}}_{k+1}^f))^{\mathrm{T}}$$

式中　$\boldsymbol{P}_{k+1}^f$——预报场误差协方差矩阵

$\boldsymbol{H}$——观测算子

$\boldsymbol{R}$——预测误差协方差矩阵

$\overline{\boldsymbol{X}}_{k+1}^f$——$k+1$ 时刻状态变量预报平均值

（4）计算 $k+1$ 时刻状态变量分析值 $\boldsymbol{X}_{k+1}^a$ 与分析场误差方差矩阵 $\boldsymbol{P}_{k+1}^a$ 分别为

$$\boldsymbol{X}_{k+1}^a = \boldsymbol{X}_{k+1}^f + \boldsymbol{K}_{k+1}[(\boldsymbol{Y}_{k+1} + \boldsymbol{\nu}_{k+1}) - \boldsymbol{H}(\boldsymbol{X}_{k+1}^f)] \quad (\boldsymbol{\nu}_{k+1} \sim N(0, R)) \tag{4}$$

$$\boldsymbol{P}_{k+1}^a = \frac{1}{N-1} \sum_{i=1}^{N} (\boldsymbol{X}_{k+1}^a - \overline{\boldsymbol{X}}_{k+1}^a)(\boldsymbol{X}_{k+1}^a - \overline{\boldsymbol{X}}_{k+1}^a)^{\mathrm{T}} \tag{5}$$

其中

$$\overline{\boldsymbol{X}}_{k+1}^a = \frac{1}{N} \sum_{i=1}^{N} \boldsymbol{X}_{k+1}^{ai} \tag{6}$$

式中　$\boldsymbol{Y}_{k+1}$——$k+1$ 时刻的状态变量的观测值

$\boldsymbol{\nu}_{k+1}$——期望为 0、方差为 $\boldsymbol{R}$ 的高斯白噪声

（5）判断是否到结束时刻，即目标年份。如果未到结束时刻，则返回步骤（2），否则结束。

1.4.2　EnKF 与 CA/Markov 模型实现

利用集合卡尔曼滤波数据同化算法融合高分辨率遥感影像源地的观测数据得出同化结果，其输入数据为非布尔型，而 CA/Markov 模型模拟元胞的结果状态只有两种，即源地与非源地[13－20]。故将整个研究区划分为若干个正方格区域，每个方格里有若干个像元（元胞），得出每一个方格内的源地元胞扩张强度。

元胞扩张强度 Ω_{ij}^t 的计算式为

$$\Omega_{ij}^t = \frac{\sum_{m \times m} con(s_{ij} = source)}{mm} \tag{7}$$

式中　$con(s_{ij} = source)$——区域内源地元胞的数量

此时，方格内的元胞总个数为 $m \times m$，每个方格内有一个扩张强度，令 EnKF 中的 $\boldsymbol{X}_k^f$ 每个状态变量对应一个方格的扩张强度，通过 EnKF 的计算公式便可得出同化值 $\boldsymbol{X}_{k+1}^a$，根据同化值可修正 CA/Markov 模型模拟结果。具体包括以下步骤：①使用 CA/Markov 模型模拟到同化年份，得出每个方格的源地扩张强度模拟值。②根据模拟值与观测值设置相关的参数（如观测误差、模拟误差、集合个数等），

运用集合卡尔曼滤波的公式得出同化值(同化后各个方格的发展强度)。③根据同化值,对当前的模拟结果进行修正。

利用 ArcGIS 软件的 Fishnet 模块将全区分为 513 个规则方块,从中选出 66 个观测点和 56 个检测点(图 2)。

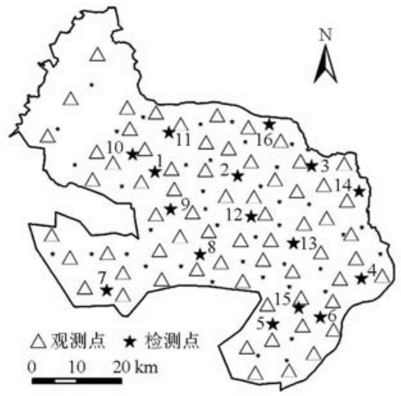

图 2 观测点与检测点空间分布图

Fig. 2 Spatial distribution of observation points and detection points

误差统计方式采用方差(V_{SE}),其计算式为

$$V_{SE}=\sum_{i=1}^{N}(y_i-x_i)^2 \tag{8}$$

式中 y——真实值

x——同化值或预测值,y 和 x 维数一致

1.5 MCRP 模型

生态用地扩展可以看作是生态绿色空间对其他用地空间的竞争性控制过程,且这种控制和覆盖必须通过克服阻力来实现[5,21-22],这样生态用地扩展就可以模拟为从源到汇克服阻力做功的水平过程[23]。基本生态阻力模型,即 MCR 模型的基本公式为

$$V_{\mathrm{MCR}}=f_{\min}\sum_{j=n}^{i=m}D_{ij}R_i \tag{9}$$

式中 V_{MCR}——最小累积阻力面值

$f_{\min}$——某土地单元对不同的生态用地取累积阻力最小值

D_{ij}——从生态用地 j 到土地单元 i 的空间距离

R_i——用地单元 i 对运动过程的阻力系数

考虑不同生态源地有不同的生态扩张能力,即不同生态源地的影响力是不同的,引入不同等级生态源地的扩张能力因子 P_j,修正 MCR 模型,为简化计算,按照生态源地斑块的面积对生态源地进行分级,并赋予扩张能力值。

利用 EnKF-CA/Markov 模型预测 2017 年的生态源地,利用 EnKF 算法将预测的 2017 年的生态源地与 2012 年的现状生态源地进行数据同化,得到同化后的生态源地空间分布值,该值既包含 2012 年的生态源地信息,又包含生态源地的未来变化趋势,即将源地的变化引入到生态阻力模型中。

修正后建立源地扩张能力约束下的生态阻力模型——MCRP 模型(Minimal cumulative resistance power)考虑了生态用地扩张的 4 方面因素,即生态源地变化、生态源地等级、距离和基面阻力特征,修正后公式为

$$V_{\mathrm{MCR}}P=f_{\min}\sum_{j=n}^{i=m}D_{ij}R_iP_j \tag{10}$$

式中 V_{MCRP}——生态用地扩展最小生态累积阻力面值

P_j——生态用地 j 所属等级的扩张能力因子

生态用地的等级越高,扩张能力越强。

2 结果与分析

2.1 源地变化模拟与分级

根据 2002、2007、2012 年影像解译数据结合磴口县实际情况提取生态源地,在荒漠绿洲区,湿地的生态作用巨大,故将所有水域提取出来均作为源地,在磴口县荒漠灌林地的防风固沙作用显著,生态作用十分重要,故将面积大于 0.1 km^2 的荒漠灌林地提取出来作为源地。

利用 EnKF 以 CA/Markov 模型为数据同化算子模拟源地的时空演变,集合大小设为 30,数据同化算子参数主要包括距离因子、地形因子、水文因子,如图 3 所示。

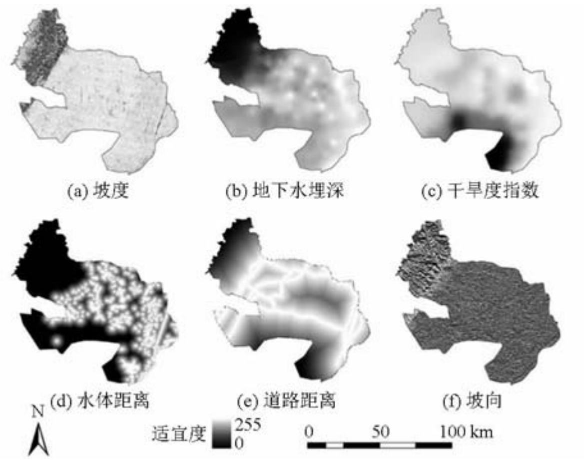

图 3 各类适宜性因子评价图

Fig. 3 Evaluation of various types of suitability factors

分别利用 CA/Markov 模型和 EnKF-CA/Markov 模型,基于 2002、2007 年的源地数据,预测 2012 年的源地空间分布(图 4b、4c),与 2012 年的生态用地实际情况进行对比验证(图 4a)。

利用 IDRISI 软件进行逐像元对比分析得出 EnKF-CA/Markov 模型的模拟总精度为 82.4%,模拟结果方差为 0.6,Kappa 系数为 0.513。传统 CA/Markov 模型的模拟总精度为 65.4%,模拟结果方差

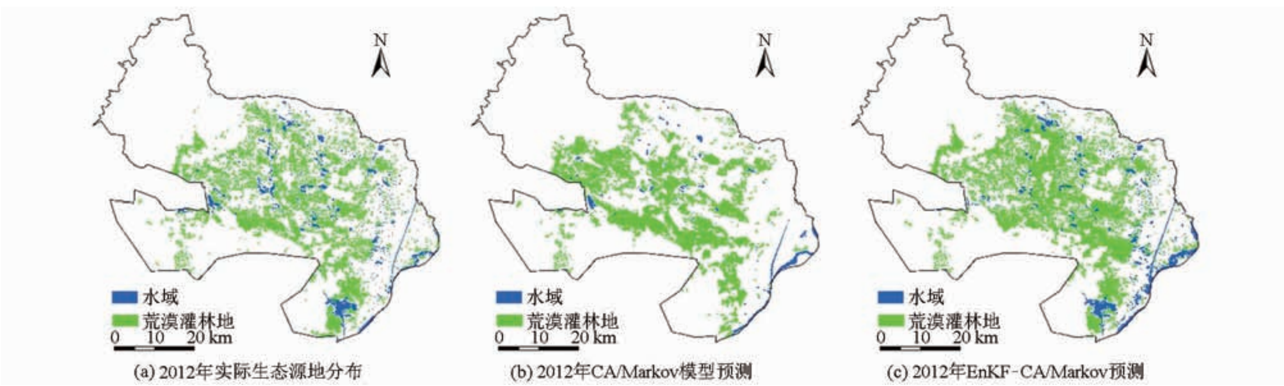

图 4　2012 年生态源地实际与模型模拟空间分布图

Fig. 4　Actual and model simulated spatial distribution map of ecological source in 2012

为 1.3，Kappa 系数为 0.342。在模拟过程中，利用数据同化技术修正的模拟结果在精度与方差上都有改善，本研究通过引入集合卡尔曼滤波，模型能够减少误差的积累，提高模拟精度。

利用 EnKF－CA/Markov 模型，基于 2007、2012 年的源地预测 2017 年的源地空间分布情况，得到 2017 年源地空间分布如图 5a 所示。将 2017 年的生态源地作为 EnKF 模型的观测值，与 2012 年的实际生态源地进行数据同化，得到 2017、2012 年的生态源地同化数据（图 5b），其中既包括 2012 年的生态源地信息，也包含生态用地变化至 2017 年的变化趋势。

进而根据源地扩展能力，对源地进行等级划分，共分为 5 个等级（图 5c），级别越高表明源地的扩张能力因子越大，5 级源地主要分布在磴口县包勒浩特嘎查、巴音温都尔嘎查、温都尔毛道嘎查、乌兰布和农场耕地外围，自磴口县东北贯穿至磴口县西南，与奈伦湖相连。4 级生态源地主要分布在巴音博日那嘎查、哈腾套海农场、纳林套海农场的耕地外围。3 级生态源地主要分布在磴口县防沙林场、奈伦湖、包尔盖农场附近。3、4、5 级生态源地的空间布局形成东北-西南、西北-西南的沙漠化防护格局，对于防治乌兰布和沙漠的扩张具有重要意义。

2.2　生态阻力面构建

由于基面特性差异，生态用地在扩张过程中所受的阻力是不同的，阻力系数反映了生态用地控制和覆盖其他用地类型难易程度。将基面阻力分为 2 类：生态障碍和生态阻力。生态障碍是生态用地无法扩展到的地块，如建设用地、基本农田等，构成生态用地扩张的刚性约束，阻力系数无穷大。生态阻力是对生态用地扩张有不同等级阻碍作用的地块，考虑地块表面的固有属性和附加属性构建了生态阻力评价体系，将生态阻力分为 5 个等级，1 级表示阻力最小，5 级表示阻力最大。固有属性包括用地类型和地质地貌特征。附加属性包括生态系统服务价值和 NDVI－水体距离。所构建的阻力评价体系如表 1、2 所示。

首先确定生态用地空间扩张障碍，第①类是基本农田，是保证磴口县区域经济、社会稳定的保障，面积为 796.28 km^2。第②类是建设用地，是生态用地扩张的刚性限制。生态障碍分布图如图 6a 所示。

进而确定生态阻力面，根据生态阻力评价体系，使用 MCRP 模型算法，利用 ArcGIS 软件中的 cost－distance 模块分别生成 5 个等级源地生态阻力面，进行叠加计算生成生态用地扩张生态阻力面，如图 6b 所示，累计阻力值最小为 0，位于生态用地内部，累

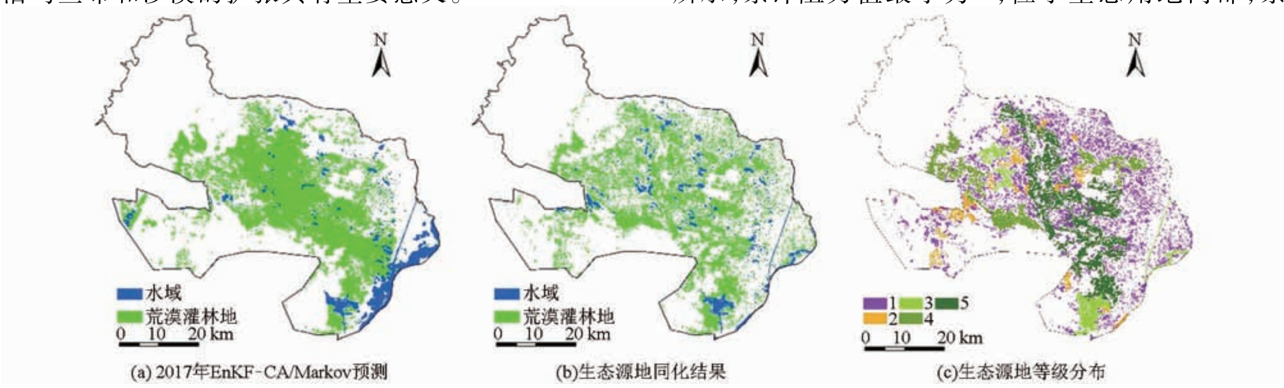

图 5　生态源地及等级划分空间分布图

Fig. 5　Distribution map of ecological sources and classification of space

表 1 生态阻力评价体系

Tab. 1 Evaluation system of ecological resistance

项目	属性值				
	1	2	3	4	5
用地类型	天然湖泊、水库坑塘、河流沟渠等	荒漠灌林、城镇绿地、天然牧草地等	耕地	城镇与建设用地	沙漠
地形地貌	极软基质	低软基质	柔软基质	低硬基质	坚硬基质
服务功能	供水、防洪、排水、水净化、二氧化碳吸收和氧气释放	防风、阻止沙漠化、野生动物栖息地	维护生物多样性、生物量生产	为人类居住提供土地	

表 2 NDVI 与水体距离生态阻力评价体系

Tab. 2 Evaluation system of ecological resistance between NDVI and water distance

NDVI	与水体之间的距离/km				
	0 ~ 30	30 ~ 60	60 ~ 120	120 ~ 180	大于 180
0.8 ~ 1.0	1	1	2	2	2
0.6 ~ 0.8	1	2	2	3	3
0.4 ~ 0.6	2	3	3	4	4
0.2 ~ 0.4	2	3	4	4	4
0 ~ 0.2	3	4	5	5	5

计阻力值最大为 77 780.8，位于乌兰布和沙漠内部。由累计阻力面可以看出，生态用地外围阻力均较大，形成明显的累计阻力“山脊线”，这是由于在荒漠灌林地外围是大面积的沙漠，累计阻力低的区域较为破碎，整体性差，严重影响景观流的流动。干旱区由于生态环境脆弱，荒漠化严重使得景观生态流流动不畅，固有属性导致其景观流阻力较大，而城市化的加剧导致了人工不透水表面的增加，进一步加剧了景观破碎，增加了景观流动阻力。

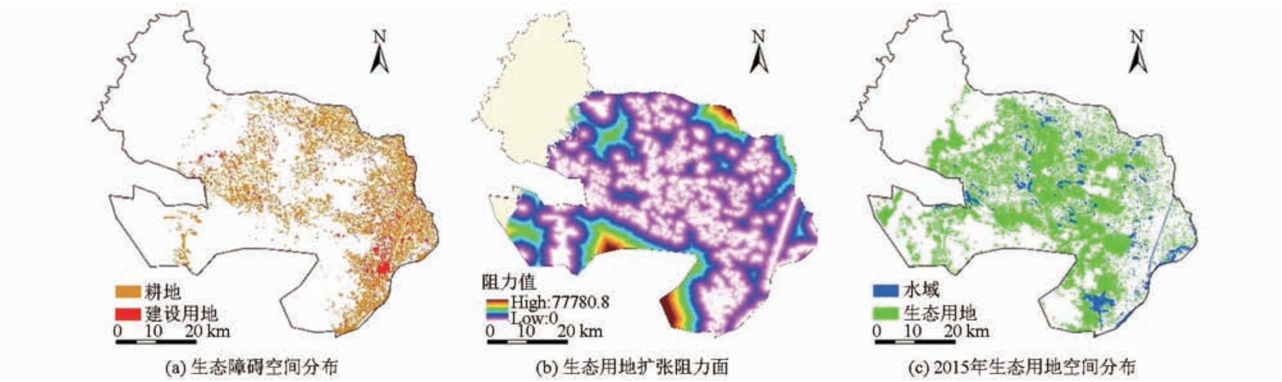

图 6 生态障碍、阻力面及 2015 年生态用地空间分布图

Fig. 6 Ecological barrier, resistance surface and spatial distribution of ecological land in 2015

2.3 生态用地扩张模拟

利用 ArcGIS 10.2 软件，使用 python 脚本语言编写程序实现模型的模拟。以 2012 年为基期数据，设置时间阈值为 3 a，分别使用 2012 年实际生态源地、经过数据同化后的生态源地数据，利用生成的阻力面使用 MCR 模型和 MCRP 模型分别进行生态用地扩张模拟，即模拟得出至 2015 年时的生态用地情况（图 6c），为便于验证，以 2015 年的生态用地面积为检验标准，磴口县 2015 年的湿地型生态用地共 137.92 km^2。荒漠植被型、天然绿洲型、城镇绿洲型、夹荒地型生态用地总计为 1 042.96 km^2。

经过迭代计算，利用 EnKF - MCRP 模型模拟的 2015 年生态用地面积共 1 260.95 km^2（图 7a），MCRP 模型模拟的生态用地面积为 983.57 km^2（图 7b），EnKF - MCR 模型模拟的生态用地面积为 1 631.35 km^2（图 7c）。与 2015 年的实际生态用地面积相对比，利用数据同化技术加入多时期生态源地变化的 MCRP 模型精度最高，逐像元对比方差为 0.4，且整体的生态用地空间布局接近实际情况，利用 MCRP 模型的模拟精度其次，方差为 1.7。考虑生态源地的变化后，MCRP 模型模拟结果比 2015 年生态用地真实面积略大，不使用数据同化技术的 MCRP 模型模拟结果要比实际偏小，说明数据同化技术能够提高模型模拟精度，将生态源地的变化作为模型因素十分必要。与 EnKF - MCRP 模型相比，EnKF - MCR 模型的模拟结果精度较低，逐像元对比方差为 3.1，模拟面积比真实值高 450.37 km^2，表明在构建生态阻力面时一方面要考虑不同等级源地的生态阻力，另一方面要考虑生态障碍的刚性限制，由模拟结果图可知，未考虑生态障碍的生态用地扩张中明显侵占了基本农田和建设用地。

对 56 个检测点的用地类型与实际用地类型进行对比验证，其中相一致的赋值为 1，不一致的赋值为 2，56 个检测点的用地类型一致性对比发现，

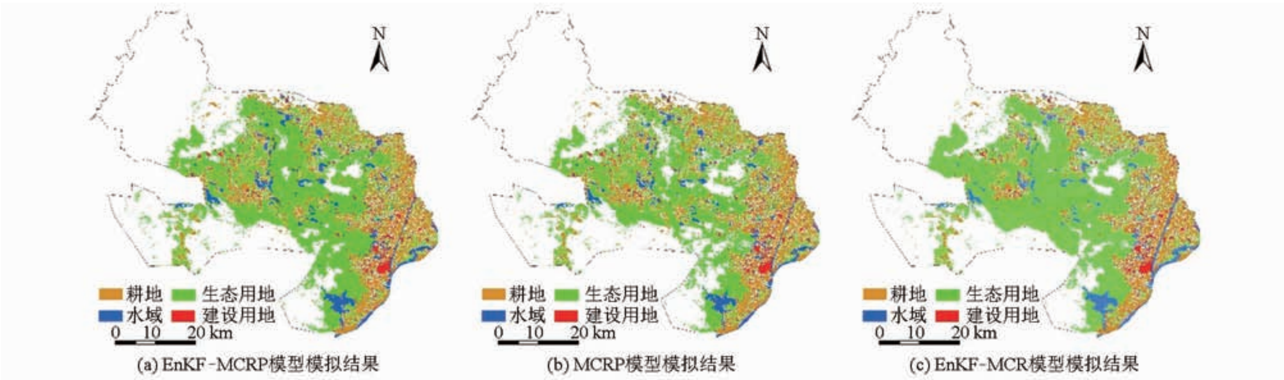

图 7　生态用地模型模拟空间分布图

Fig. 7　Spatial distribution map of ecological land use through model simulation

EnKF－MCRP 模型模拟结果与实际情况相符程度最高，MCRP 模拟结果有 11 个点与实际不一致，EnKF－MCR 模拟结果有 19 个点与实际不一致。

在 56 个检测点中选出 16 个具有代表性的检测点并对其模拟结果进行重点分析（表 3），其中检测点 1、3、4、5、6、11、14、15、16 处 EnKF－MCRP、MCRP、EnKF－MCR 模型的模拟结果均与实际相符合，经过同化作用后，同化的结果较明显，特别是检测点 2，2015 年检测点 2 处为生态用地，EnKF－MCRP、EnKF－MCR 模型的模拟结果与实际相符，但是 MCRP 模型模拟结果与实际不符合，表明数据同化对于模拟精度的提高作用明显，检测点 10、12 位于生态用地的边缘，结合数据同化技术的模型模拟结果均与实际相符合，未利用数据同化技术的 MCRP 模型模拟结果则精度较低，若迭代年份改变可能会导致模拟结果错误，总体来看，整个同化过程中各点均能从观测点中获取正确的增益信息，因而能够得出一个较好的误差相关矩阵，作用到增益矩阵中，从而得出较好的同化值。所以数据同化能够根据观测点的信息得出比模拟值更接近真实值的同化值。故引入集合卡尔曼滤波的数据同化方法到模型中，能取得比较好的模拟结果。检测点 7、8、9 处于生态障碍中，检测点 13 位于生态障碍边缘，EnKF－MCRP、MCRP 模型的模拟结果均与实际相符，EnKF－MCR 模型的模拟结果为生态用地，表明生态用地发生了过度扩张，在构建生态阻力面模型时考虑不同等级生态源地的生态障碍十分必要。

表 3　部分检测点用地类型

Tab. 3　Land type for some detection points

检测点	EnKF－MCRP	MCRP	EnKF－MCR	2015 年实际	位置
1	1	1	1	1	内部
2	1	4	1	1	内部
3	1	1	1	1	边缘
4	2	2	2	2	内部
5	3	3	3	3	内部
6	2	2	2	2	内部
7	2	2	1	2	边缘
8	2	2	1	2	边缘
9	2	2	1	2	边缘
10	1	1	1	1	边缘
11	3	3	3	3	内部
12	1	1	1	1	内部
13	2	2	2	2	边缘
14	2	2	2	2	内部
15	1	1	1	1	内部
16	1	1	1	1	边缘

注：1 为生态用地，2 为生态障碍，3 为沙漠，4 为非生态用地。

3　结论

（1）磴口县生态源地包括湿地型生态用地和荒漠植被型生态用地，生态源地对于维持区域生态用地稳定发展有重要作用。本文将数据同化技术应用于生态源地的变化模拟中，将生态源地的变化趋势量化，EnKF－CA/Markov 模型的模拟总精度达到 82.4%，通过引入集合卡尔曼滤波，能够减少误差的积累，提高模拟的精度。

（2）根据生态源地的扩展能力，将磴口县生态源地划分为 5 个等级，研究表明：磴口县的 3、4、5 级生态源地的空间布局形成东北－西南、西北－西南的沙漠化防护格局，对于防治乌兰布和沙漠的扩张具有重要意义，对于维持区域生态环境稳定具有重大作用。

（3）在构建生态阻力面时考虑生态障碍和生态阻力两个方面，将生态障碍引入阻力面构建中能够防止生态用地的过度扩张，考虑生态源地变化、生态源地等级、距离、基面阻力 4 方面构建 MCRP 模型，累计阻力值最小为 0，最大为 77 780.8，生态障碍阻力为无穷大。结果表明引入数据同化技术的 EnKF－MCRP 模型的生态用地扩张模拟精度最高，生态用地面积与空间布局最接近实际情况，数据同化对于模拟精度的提高作用明显。

参 考 文 献

1 周锐,王新军,苏海龙,等.平顶山新区生态用地的识别与安全格局构建[J].生态学报,2015,35(6):2003-2012.
ZHOU Rui, WANG Xinjun, SU Hailong, et al. Identification and security pattern of ecological land in Pingdingshan newly developed area[J]. Acta Ecologica Sinica,2015,35(6):2003-2012.(in Chinese)

2 张红旗,王立新,贾宝全.西北干旱区生态用地概念及其功能分类研究[J].中国生态农业学报,2004,12(2):5-8.
ZHANG Hongqi, WANG Lixin, JIA Baoquan. A conception of ecological land use and its function classification in arid area in Northwest China[J]. Chinese Journal of Eco-Agriculture,2004,12(2):5-8.(in Chinese)

3 岳德鹏,王计平,刘永兵,等.京郊西北地区农地利用与景观格局时空特征[J].农业工程学报,2008,24(6):89-95.
YUE Depeng, WANG Jiping, LIU Yongbing, et al. Spatial and temporal characteristics of agricultural land-use and landscape pattern changes in northwest of Beijing[J]. Transactions of the CSAE,2008,24(6):89-95.(in Chinese)

4 梁曼,孙璇,杨振.土地景观生态流空间通达性评价——以荆州市为例[J].河南科学,2014,32(8):1654-1658.
LIANG Man, SUN Xuan, YANG Zhen. Evaluation on spatial accessibility of ecological circulation of landscape—a case of Jingzhou City[J]. Henan Science,2014,32(8):1654-1658.(in Chinese)

5 叶玉瑶,苏泳娴,张虹鸥,等.生态阻力面模型构建及其在城市扩展模拟中的应用[J].地理学报,2014,69(4):485-496.
YE Yuyao, SU Yongxian, ZHANG Hong'ou, et al. Ecological resistance surface model and its application in urban expansion simulations[J]. Acta Geographica Sinica,2014,69(4):485-496.(in Chinese)

6 YU Q, YUE D P, WANG J P, et al. The optimization of urban ecological infrastructure network based on the changes of county landscape patterns: a typical case study of ecological fragile zone located at Deng Kou (Inner Mongolia)[J]. Journal of Cleaner Production, doi: 10.1016/j.jclepro.2016.05.014.

7 LI F, Ye Y P, SONG B W. Evaluation of urban suitable ecological land based on the minimum cumulative resistance model: a case study from Changzhou, China[J]. Ecological Modelling,2015,318:194-203.

8 张亦汉,黎夏,刘小平,等. 基于数据同化的元胞自动机[J].遥感学报,2011,15(3):475-491.
ZHANG Yihan, LI Xia, LIU Xiaoping, et al. The CA model based on data assimilation[J]. Journal of Remote Sensing,2011,15(3):475-491.(in Chinese)

9 桂预风,纪元,杨慧. 基于粒子滤波的随机元胞自动机城市用地扩张模型研究[J].数学的实践与认识,2015,45(17):222-227.
GUI Yufeng, JI Yuan, YANG Hui. The research of urban sprawl with the stochastic cellular automata model based on particle filter [J]. Mathematics in Practice and Theory,2015,45(17):222-227.(in Chinese)

10 张生雷,陈良富,苏林,等.一种基于数据同化优化陆面过程模式参数化方案的方法[J].中国科学:地球科学,2015,45(12):1907-1922.
ZHANG Shenglei, CHEN Liangfu, SU Lin, et al. A data assimilation-based method for optimizing parameterization schemes in a land surface process model[J]. Science China: Earth Sciences,2015,45(12):1907-1922.(in Chinese)

11 黄健熙,李昕璐,刘帝佑,等. 顺序同化不同时空分辨率 LAI 的冬小麦估产对比研究[J].农业机械学报,2015,46(1):240-248.
HUANG Jianxi, LI Xinlu, LIU Diyou, et al. Comparison of winter wheat yield estimation by sequential assimilation of three different spatial-temporal resolution remotely sensed LAI datasets[J]. Transactions of the Chinese Society for Agricultural Machinery,2015,46(1):240-248.(in Chinese)

12 李保杰.矿区土地景观格局演变及其生态效应研究——以徐州市贾汪矿区为例[D].徐州:中国矿业大学,2014.
LI Baojie. Study on landscape pattern changes and ecological effects in mining area—A case study in Jiawang mining area [D]. Xuzhou: China University of Mining and Technology,2014.(in Chinese)

13 张亦汉,乔纪纲,艾彬.基于集合卡尔曼滤波动态优化 CA 模型参数的方法[J].测绘学报,2013,42(1):123-130.
ZHANG Yihan, QIAO Jigang, AI Bin. Parameter optimization for CA model using ensemble Kalman filter[J]. Acta Geodaetica et Cartographica Sinica,2013,42(1):123-130.(in Chinese)

14 王文,刘永伟,寇小华,等.基于集合卡尔曼滤波和 HYDRUS-1D 模型的土壤剖面含水量同化试验[J].水利学报,2012,43(11):1302-1311.
WANG Wen, LIU Yongwei, KOU Xiaohua, et al. EnKF and HYDRUS-1D based data assimilation experiments for improving soil moisture profile prediction[J]. Journal of Hydraulic Engineering,2012,43(11):1302-1311.(in Chinese)

15 李渊,基于数据同化的太湖叶绿素浓度遥感估算[D].南京:南京师范大学,2014.
LI Yuan. Chlorophyll a concentration remote evaluation in Lake Taihu based on data assimilation[D]. Nanjing: Nanjing Normal University,2014.(in Chinese)

16 高斌斌.集合 Kalman 滤波在 T106L19 中期数值预报谱模式中的应用研究[D].南京:南京信息工程大学,2008.
GAO Binbin. Application research on the ensemble Kalman filter (EnKF) with a medium-range numerical weather prediction (NWP) spectral model at a T106L19 resolution[D]. Nanjing: Nanjing University of Information Science & Technology, 2008.(in Chinese)

17 HALMY M W, GESSLER P E, HICKE J A, et al. Land use/land cover change detection and prediction in the north-western

coastal desert of Egypt using Markov-CA[J]. Applied Geography,2015,63:101 －112.

18 张滢,丁建丽.绿洲土地利用变化未来趋势预测及其调控研究[J].干旱区资源与环境,2006,20(6):29 －35.
ZHANG Ying, DING Jianli. Study on forecasting and regulation of future trend of oasis land use[J]. Journal of Arid Land Resources and Environment,2006,20(6):29 －35.(in Chinese)

19 王友生,余新晓,贺康宁,等.基于 CA－Markov 模型的藉河流域土地利用变化动态模拟[J].农业工程学报,2011,27(12):330 －336.
WANG Yousheng, YU Xinxiao, HE Kangning, et al. Dynamic simulation of land use change in Ji He watershed based on CA－Markov model[J]. Transactions of the CSAE,2011,27(12):330 －336.(in Chinese)

20 赵冬玲,杜萌,杨建宇,等. 基于 CA－Markov 模型的土地利用演化模拟预测研究[J].农业机械学报,2016,47(3):278 －285.
ZHAO Dongling, DU Meng, YANG Jianyu, et al. Simulation and forecast study of land use change based on CA－Markov model [J]. Transactions of the Chinese Society for Agricultural Machinery,2016,47(3):278 －285.(in Chinese)

21 尹发能.江汉平原四湖流域景观生态规划与流域生态管理研究[D].上海:华东师范大学,2008.
YIN Faneng. Study of landscape ecological Planning and drainage basin ecological management in the Four-Lake basin[D]. Shanghai:East China Normal University,2008.(in Chinese)

22 RAY N, LEHMANN A, JOLY P. Modeling spatial distribution of amphibian populations: a GIS approach based on habitat matrix permeability[J]. Biodiversity & Conservation,2002,11(12):2143 －2165.

23 HERZOG F, LAUSCH A, MULLER E, et al. Landscape metrics for assessment of landscape destruction and rehabilitation[J]. Environmental Management,2001,27(1):91 －107.